Remote Sensing of Environment 112 (2008) 4061–4074

Contents lists available at ScienceDirect

Remote Sensing of Environment

journal homepage: www.elsevier.com/locate/rse

Wetland change mapping for the U.S. mid-Atlantic region using an outlier detection technique

Eric M. Nielsen [a,*], Stephen D. Prince [a], Gregory T. Koeln [b]

[a] Department of Geography, University of Maryland, College Park, MD 20942, USA
[b] MDA Federal Inc., Rockville, MD 20852, USA

ARTICLE INFO

Article history:
Received 31 March 2007
Received in revised form 24 April 2008
Accepted 26 April 2008

Keywords:
Remote sensing
Wetlands
Mid-Atlantic U.S.
Chesapeake Bay
Change detection
Marsh degradation
Resistant z-score
Phragmites australis

ABSTRACT

Although the impacts of wetland loss are often felt at regional scales, effective planning and management require a comparative assessment of local needs, costs, and benefits. Satellite remote sensing can provide spatially explicit, synoptic land cover change information to support such an assessment. However, a common challenge in conventional remote sensing change detection is the difficulty of obtaining phenologically and radiometrically comparable data from the start and end of the time period of interest. An alternative approach is to use a prior land cover classification as a surrogate for historic satellite data and to examine the self-consistency of class spectral reflectances in recent imagery. We produced a 30-meter resolution wetland change probability map for the U.S. mid-Atlantic region by applying an outlier detection technique to a base classification provided by the National Wetlands Inventory (NWI). Outlier-resistant measures – the median and median absolute deviation – were used to represent spectral reflectance characteristics of wetland class populations, and formed the basis for the calculation of a pixel change likelihood index. The individual scene index values were merged into a consistent region-wide map and converted to pixel change probability using a logistic regression calibrated through interpretation of historic and recent aerial photography. The accuracy of a regional change/no-change map produced from the change probabilities was estimated at 89.6%, with a Kappa of 0.779. The change probabilities identify areas for closer inspection of change cause, impact, and mitigation potential. With additional work to resolve confusion resulting from natural spatial heterogeneity and variations in land use, automated updating of NWI maps and estimates of areal rates of wetland change may be possible. We also discuss extensions of the technique to address specific applications such as monitoring marsh degradation due to sea level rise and mapping of invasive species.

1. Introduction

1.1. Wetlands and the need for monitoring

Wetlands perform a wide range of stabilizing functions, including water quality protection through particulate and nutrient retention, minimization of flooding and erosion, maintenance of stream flow, and recharging of groundwater (Tiner, 2003). The high productivity of many wetlands supports diverse, unique, and economically important biological communities (Gibbs, 2000). The spatial arrangement of intact wetlands is important, as they provide habitat cores and corridors that assist in maintaining the diversity of entire landscapes and can form cornerstone elements for regional conservation strategies (Weber, 2004).

Although wetlands are inherently dynamic systems and are created, modified, and destroyed by a range of natural processes, the direct or indirect consequences of human activity are the main cause of wetland change and loss in the United States. Less than half the wetland acreage that existed at the time of European settlement remains (Dahl, 2006). Urban and agricultural expansion have driven extensive wetland filling and draining, while hydrological alterations to wetlands due to reservoir and river levee construction, marsh diking, and shore stabilization are widespread (Brinson & Malvarez, 2002; Kennish, 2002; Tockner & Stanford, 2002). Increasing nutrient and pollutant inputs due to rising populations threaten wetlands in coastal areas (Kennish, 2002), and relative sea level rise has resulted in the loss of many estuarine marshes (e.g., Morris et al., 2002; Erwin et al., 2004). The spread of invasive species has compromised the biological integrity and ecosystem functions of other wetlands (Kennish, 2002; Tockner & Stanford, 2002).

The diverse and pervasive threats to wetlands point to the need for comprehensive monitoring efforts at regional to national scales. The U.S. National Wetlands Inventory (NWI) program has undertaken

* Corresponding author. Remote Sensing Applications Center, USDA Forest Service, 2222 W 2300 S, Salt Lake City, UT 84119, USA. Tel.: +1 801 975 3761; fax: +1 801 975 3478.
E-mail address: emnielsen@fs.fed.us (E.M. Nielsen).

0034-4257/$ – see front matter © 2008 Elsevier Inc. All rights reserved.
doi:10.1016/j.rse.2008.04.017

this task for the continental U.S. in their Wetland Status and Trends (WST) reports. The most recent (Dahl, 2006) provides sample-based aggregated nationwide change rate estimates for major wetland types during the time period 1998–2004. Although the analysis indicated a net expansion of wetland area during these years, the increase was primarily due to the widespread construction of freshwater ponds. Because artificial ponds provide few of the benefits associated with natural vegetated wetlands, the total area occupied by wetlands can be a misleading statistic. Natural vegetated wetlands continue to be eliminated, although at a considerably lower rate than they were prior to the mid-1970s (Dahl, 2006).

Although national trends in the prevalence of various wetland types are useful, many applications (e.g., ecosystem modeling, conservation planning) need information on the spatial distribution of wetland modification and loss. Koneff and Royle (2004) used kriging to produce a continuous change map at 2-mile resolution based on the image- and field-interpreted samples provided by a previous WST study. While their approach produced good results for some wetland types, other types were problematic, likely due to the high level of spatial variability in the distribution of agricultural, forestry, and development activities in the mid-Atlantic region (Koneff & Royle, 2004). Kearney et al. (2002), assessing coastal marsh losses in the Chesapeake and Delaware Bays, concluded that comprehensive spatially explicit analyses are needed to address unpredictable regional variations in the processes driving wetland degradation. Synoptic change estimates could also be applied to inherently spatial landscape-level problems such as assessment of trends in water quality and wildlife habitat suitability.

1.2. Wetland mapping

Wetland identification via satellite-based optical remote sensing is well-represented in the literature (e.g., Sader et al., 1995; Lunetta & Balogh, 1999; reviewed by Ozesmi & Bauer, 2002) despite the special challenges presented. Standing water and the soil surface can be obscured by vegetation, and most wetlands experience fluctuations in flooded extent and water depth and turbidity (Rundquist et al., 2001). Seasonal and inter-annual environmental change create variability in inland wetlands, while the tidal cycle causes rapid changes in the apparent extent of coastal wetlands (Pavri & Aber, 2004). The high productivity of vegetation in many wetland environments often translates into large inter-seasonal fluctuations in actively photosynthesizing leaf area. The small size and fine-scale heterogeneity of many wetlands create additional challenges in the use of imagery collected at mid- to coarse spatial resolutions (Ramsey & Laine, 1997).

Wetlands can, however, be effectively mapped from an aerial photography or high resolution satellite imagery (Dahl, 2006). Imagery can be acquired at a phenologically optimal date, and human interpreters can identify and classify wetlands that would be missed by the most sophisticated automated procedures. The NWI has used aerial photography, soils and topographic maps, and fieldwork to interpret, classify, and map most wetlands in the conterminous U.S. (Wilen & Bates, 1995). This one-time comprehensive effort can be used as a baseline for change detection, but photointerpretation is impractical for ongoing monitoring over large areas due to flight time and data processing expenses. Moderate resolution satellite imagery, while insufficient for detailed wetland classification, is well suited to regional scale monitoring tasks and represents a good compromise between resolving power, spatial coverage, and expense.

1.3. Wetland change detection

In general, remote sensing change detection approaches based on image differencing (including use of transformations such as principal components analysis, spectral mixture modeling, and various vegetation indices, and extensions such as change vector analysis) have been found to be most effective at mapping land cover change (see Lu et al., 2004). The NOAA Coastal Change Analysis Program (C-CAP; Dobson et al., 1995), a major national U.S. wetlands change mapping program, therefore recommends image differencing to isolate changed areas for subsequent reclassification. However, image differencing in wetlands is affected by many of the same issues of natural variability that impact mapping. While changes in vegetation phenology can be minimized through the use of anniversary imagery, hydrological variability is as significant as a cause of confusion and is far less manageable. The high level of natural temporal variability in wetlands is a serious constraint on the use of simple image differencing techniques.

Image differencing is also impractical when the map to be updated is older than the time period covered by the usable sensor data records. In the U.S., the mean size of emergent wetland patches converted to agriculture is about 1.6 ha (Dahl, 2006). This is within the detection capabilities of the Landsat Thematic Mapper (TM) sensors, whose data record stretches back to 1982. However, many parts of the country were mapped by NWI before that date, in an era from which satellite imagery of sufficient spatial resolution and suitable for regional analyses is extremely limited or non-existent. The alternative utilized here is to use a classified map derived from earlier work as a surrogate for historic imagery and to examine the internal consistency of the mapped classes in the spectral reflectance space provided by recent satellite imagery. We suggest that this may be a fruitful approach for change detection applications in other highly variable land cover types and in studies spanning time periods predating the usable satellite imagery record.

1.4. Outlier detection

Change detection can be accomplished by using a prior classified map as a guide and examining the spectral reflectance variability within each mapped class using recent remotely sensed imagery. For most land cover types, atypical pixels can be fairly assumed to have changed (or in some cases to have been mapped incorrectly in the first place). A pixel's change likelihood can be expressed as a continuous variable based on its departure from some measure of reflectance central tendency for all pixels in its class. The statistical *z*-score or "normal deviate" (Zar, 1996), representing the standardized distance of a sample from the population mean, is a simple way to express this relative deviation. By restricting analysis to pixels assigned to a class of interest from an earlier map, a spatially explicit and comprehensive index of change relative to that base map can be produced. Mathematically, this technique is no different from the commonly used image processing procedure of masking out irrelevant land cover classes in order to compute image statistics based on a single class of interest, for the purpose of aiding the visualization of reflectance variability within that class. A key assumption here is that the map classes effectively segregate pixels likely to undergo processes of inherent variability as a coherent group, enabling separation of real change from natural variations that would be flagged as apparent change by a standard image differencing procedure.

Houhoulis and Michener (2000) used a *z*-score-based technique to label wetland change polygons on the coastal plain of Georgia. They conducted their analysis on a spectral "brightness" variable defined as the summed Euclidean magnitude of all spectral bands, which was sufficient for their purpose of detecting wetland conversion to agricultural uses. Koeln and Bissonnette (2000) developed a methodology termed "cross-correlation analysis" (CCA) that is based on the same principle. CCA was developed primarily to assist re-mapping efforts, identifying hotspots of likely change using coarse spatial resolution data that can then be reclassified using imagery of higher spatial resolution. In CCA, a Euclidean magnitude is summed from *z*-scores determined independently for the red, near-infrared, and mid-infrared TM bands, producing a positive-valued, non-directional *z*-score. Class-specific empirical thresholds are then applied to produce a discrete change map.

A complication in using this technique over a large region spanning multiple satellite images is that the relationship between a pixel's *z*-

score and its change probability is dependent on the distributional characteristics of the population to which it belongs. The z standardization – a function of the population mean and standard deviation – is itself sensitive to the presence and frequency of outliers in the population. Regional variation in outlier prevalence can therefore result either in outliers remaining undetected or in misclassification of normal observations as outliers. The confounding of the relationship between *z*-score and change probability over multiple satellite scenes which incorporate variability in real land cover change rates diminishes the simple *z*-score's utility for accurately estimating change rates and producing consistent maps over large regions.

A practical solution to this problem is the use of statistical measures that are less sensitive to the presence of outliers than the mean and standard deviation. The median and median absolute deviation (mad) provide statistical class descriptions that remain nearly unaffected by outliers except in extremely skewed populations (Jain et al., 2005) and thus allow an internally consistent mosaic to be produced across multiple satellite scenes spanning large areas. A *z*-score calculated using these outlier-resistant measures is referred to here as a "resistant *z*-score." Fig. 1 demonstrates the improvement in outlier recognition resulting from the use of thresholds based on the resistant *z*-score. The lower estimation efficiency of median-based measures can be an issue in sampling from distributions that are far from normal (Jain et al., 2005), but the use of synoptic remote sensing data obviates the need for sampling. Furthermore, we have found that the median is equivalent or superior to the mean for describing the central tendencies of the normal and log-normal reflectance distributions characteristic of specific land cover classes in optical remote sensing.

Rather than converting the resistant *z*-score to a discrete change indicator by thresholding, it can be transformed to a change probability through a logistic regression based on empirical calibration data. Maintenance of a continuous-valued indicator allows the possibility of detecting sub-pixel changes, which is important when – as in this case – the phenomenon of interest often occurs at or under the spatial resolution of the sensor (e.g., Hansen et al., 2002). A continuous output also allows the application of a variable threshold as circumstances demand later in the mapping or analysis process. The change detection process can also be enhanced by calculating signed, directional, resistant *z*-scores in dimensions defined by physically meaningful transformations of the spectral reflectance data, permitting the targeting of certain change types and allowing more direct identification of the change undergone.

These modifications and extensions to the basic *z*-score change detection technique are collectively referred to here as resistant *z*-score analysis (RZA). The basic requirements that must be met in order to successfully apply RZA are that (1) unchanged pixels of a particular mapped class should exhibit unimodal – and preferably normal or log-normal – reflectance distributions, that (2) change rates are not so high that the median and median absolute deviation become irrelevant class descriptors, and that (3) pixel classes identified in the baseline map and located on the same satellite scene undergo processes of natural variability as a coherent group. The hypothesis tested here is that RZA can consistently and accurately estimate pixel change probabilities across large regions and can therefore produce useful maps of wetland change and support determination of change rates on an areal basis.

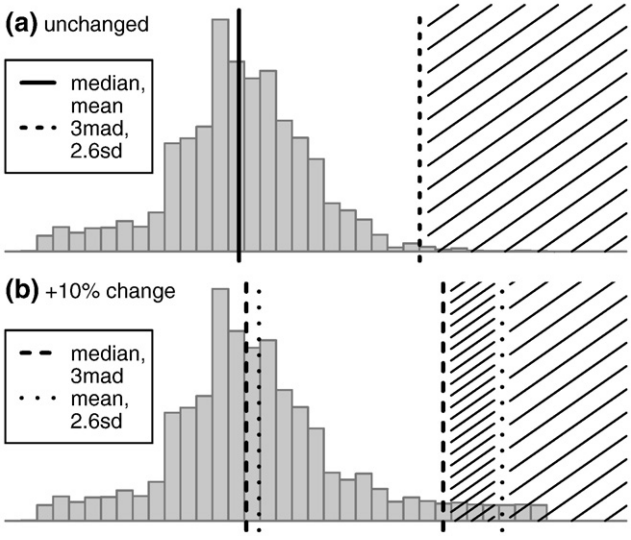

Fig. 1. Comparison of standard and resistant *z*-score methods for outlier detection. Top image (a) is the band 5 reflectance histogram of a single wetland class from one TM scene. Vertical lines represent the nearly equivalent mean and median and an upper detection threshold corresponding to 2.6 sd or 3 mad. 10% change is simulated in (b) by inserting additional high reflectance observations, half of them over the original detection threshold. The resistant 3-mad threshold is less affected by the added change than the standard 2.6-sd threshold. The standard threshold is exceeded only in the lightly hatched area, while the resistant threshold allows detection of change in the densely hatched area as well.

2. Data and methods

2.1. Study area

The study area incorporates the Chesapeake and Delaware Bay watersheds and adjacent areas (Fig. 2), where the most common wetland types are freshwater and estuarine emergent marshes and deciduous swamp forests. Of the wetland systems in the study area, palustrine wetlands are most diverse, incorporating such types as freshwater marshes of emergent herbaceous vegetation, a variety of swamp and floodplain forests, scrub-shrub swamps, and acidic bogs. The Chesapeake Bay watershed has been the focus of intensive research by the U.S. Geological Survey, Environmental Protection Agency, and other government agencies and conservation organizations. The history of wetland losses in the watershed has been reviewed by Tiner (1998). The range of data available in the region facilitates evaluation of techniques for monitoring land cover change that would not be possible in many other parts of the U.S.

2.2. TM data

We used a previously gathered three-season archive of TM data covering the study area circa year 2000. Because most wetlands exhibit pronounced changes in appearance over tidal or seasonal cycles, it is not always possible to evaluate wetland condition based on a single image. The use of multiseasonal data allowed detection of changes only apparent during a particular phenological stage, and also permitted multiple samples of the tidal cycle for coastal wetlands. Since the outlier detection process was run on a single scene at a time, it was not essential that adjacent scenes be matched in phenological stage as long as phenology was consistent within each scene. For example, variation in the green-up date of deciduous vegetation across the latitudinal range of the study area caused no problems because green-up date did not vary greatly across any single constituent TM scene. The scenes used in this study are listed in Table 1.

Pre-processing of all TM data included orthorectification and registration to precisely geolocated imagery from the Multi-Resolution Land Characteristics Consortium (RMSE<0.5 pixels) and masking of clouds, shadows, snow and ice. Masking was accomplished using a combined modeling and digitizing approach that produced conservative masks in order to minimize the impact of contamination on wetland class statistics, at the expense of the loss of some valid data on each satellite scene.

2.3. NWI data and class aggregation

NWI maps are an implementation of Cowardin et al. (1979), a hierarchical classification based on hydrological system, vegetation physiognomy, flooding regime, and substrate, supplemented by additional hydrological and water chemistry details. The maps are of varying dates and accuracy levels (Stolt & Baker, 1995; Kudray & Gale, 2000) and occasionally omit certain wetland types, primarily forests (Tiner et al., 2000; Tiner, 2003). However, their internal consistency, national scope, and availability in digital form (U.S. Fish & Wildlife Service, 2006) makes them the logical base for regional change detection work. We downloaded and merged the NWI data to assemble a wetland class code dataset for the entire study area, and converted it to raster format. Variations in mapping date and labeling detail caused some inconsistencies in the resulting mosaic, but data was available for nearly the entire study region (see Fig. 2).

We eliminated certain highly variable wetland types from the analysis, which effectively restricted the study to estuarine and palustrine wetlands. Unvegetated wetlands containing open water were removed from the analysis because they exhibited very high, spatially incoherent reflectance variability due to changes in sediment content. Wetlands with floating or submerged aquatic vegetation were likewise eliminated because of large inter-annual variability in the spatial location of their vegetative biomass. Unvegetated bare ground wetlands – mostly beaches – were also removed because minor spatial registration errors at the confluence of land and water caused unacceptable interference in the spectral analysis of these narrow wetlands. In order to additionally protect against registration error, a final phase of filtering was performed at a pixel scale, by removing from analysis any wetland pixels adjacent to upland, open water, or bare ground pixels. This had the effect of substantially reducing – sometimes to zero – the number of analyzed pixels in linear wetlands such as riparian corridors, while having minimal impact on other wetlands. Wetland loss estimates were later produced for many eliminated pixels by averaging results from adjacent non-eliminated pixels.

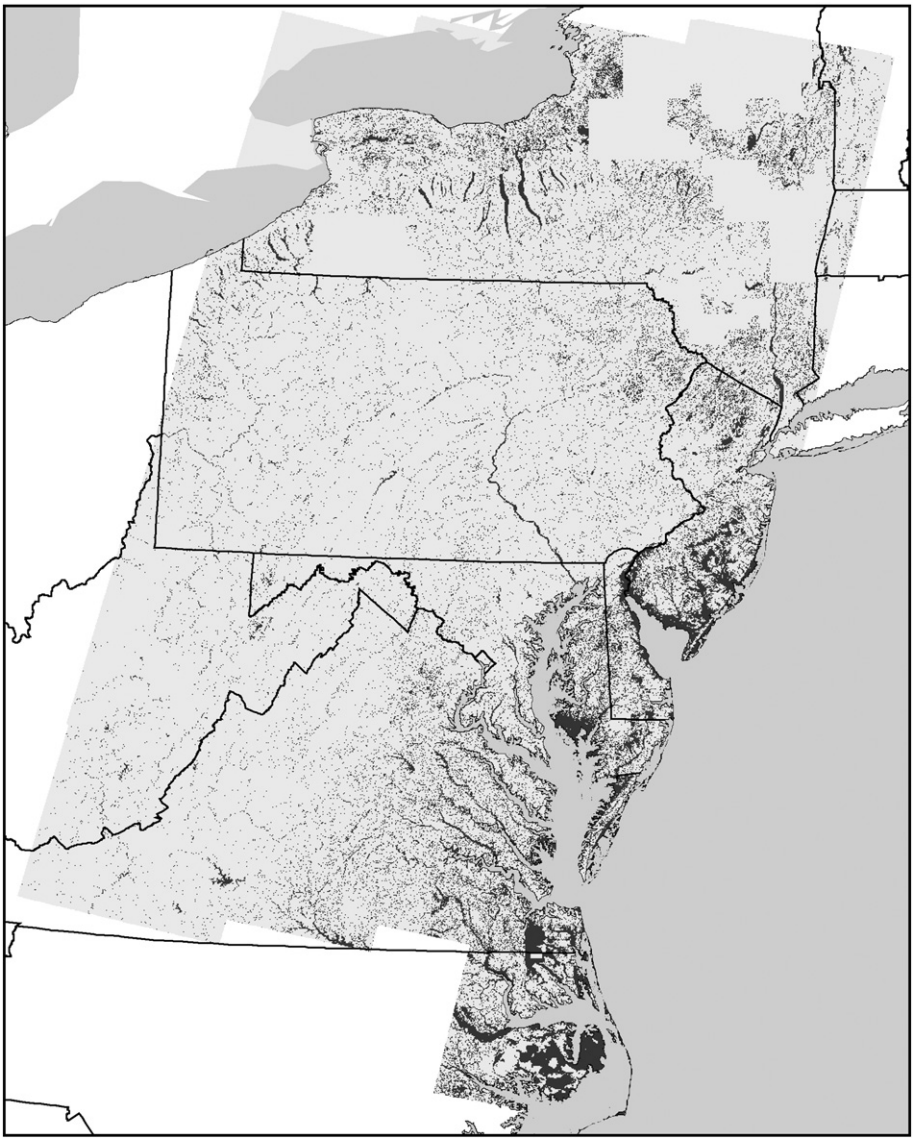

Fig. 2. Analysis was conducted on a 3-season TM image archive across the shaded region shown. NWI wetlands are superimposed; digital data were available for nearly the entire study area except for several parts of the state of New York.

After elimination of the above types, over 4500 unique NWI identifier codes remained in the study area, but many of the codes were represented by only a small number of pixels. Accurate outlier detection requires classes that contain enough pixels to permit the extraction of reliable statistical measures of spectral reflectance, and with minimal within-class natural reflectance variability. These requirements were addressed by aggregating the codes into classes that were large enough to provide reliable statistics, but that retained distinctions between all NWI-coded characteristics likely to influence spectral reflectance. The finest aggregated class in which a pixel can be placed within the limits of acceptable population size provides the most precise statistical description of its expected characteristics, and therefore allows the best opportunity for successful change detection. For example, Fig. 3 illustrates the reflectance frequency histograms pertaining to an inland, seasonally flooded emergent wetland aggregated with other wetland types at various levels of detail. The finer aggregation levels correspond to more highly specified environmental descriptions, with statistical characteristics more representative of the wetland type of interest.

Because the spectral reflectance characteristics of wetlands are primarily related to vegetation structure, leaf characteristics, and soil moisture (Brook & Kenkel, 2002), class aggregations were based on vegetation structure, leaf persistence, leaf geometry (for wooded wetlands only), wetland system, and flooding regime (see Table 2).[1] Some potentially useful characters, such as emergent wetland leaf geometry, were not used because they were only occasionally specified in the NWI data. Estuarine and palustrine wetland systems were kept separate because of their distinct vegetation and hydrological dynamics. The resulting aggregated classes were then split based on the additional hydrological details provided in the NWI codes. In general, if a substantial reduction in the size of a class could be realized by splitting, and all resulting classes still retained a sufficient number of pixels – two hundred was used as a minimum cutoff – then the split was made. For hybrid NWI codes composed of primary and secondary vegetation types, the vegetation-specific information was retained for both types.

The initial aggregation process produced a grouping of the NWI codes into 238 separate classes. However, because some classes were not adequately represented on all satellite scenes, coarser aggregations – in which wetlands were lumped into a smaller number of classes composed of a greater number of pixels each – were produced by lumping together classes which differed in terms of their hydrological modifiers and regimes, leaf geometries, and (for hybrid NWI codes) secondary vegetation types. Distinctions between vegetation physiognomies, leaf phenologies, and estuarine versus palustrine wetland systems were maintained in all cases. The three higher level aggregations totaled 100, 29, and 13 classes respectively. The characteristics used to create all aggregation levels are shown in Table 2.

The effectiveness of the aggregation scheme for variability partitioning can be evaluated by examining the evenness of the class pixel counts across the aggregated analysis classes. The cumulative distribution function illustrating the total area represented by the wetland classes in descending order of frequency is shown in Fig. 4 for the original NWI codes and for two of the aggregation levels produced here. Although a small fraction of the classes occupy most of the total wetland area in all cases, aggregation provides a more even numerical representation of the range of wetland types in the study area than the original NWI codes. Even the smallest classes produced in each aggregation retained sufficient numbers of pixels for adequate characterization on most TM scenes.

[1] The simplest classification used was an aggregation composed of 6 estuarine classes (persistent emergents, emergents with unknown phenology, deciduous forest, evergreen forest, deciduous shrub, and evergreen shrub) and 7 palustrine classes (persistent emergents, non-persistent emergents, emergents with unknown phenology, deciduous forest, evergreen forest, deciduous shrub, and evergreen shrub).

2.4. Resistant z-score analysis

TM bands 3 (visible red), 4 (near-IR), and 5 (mid-IR) were used in the analysis. These bands have been found to be the most useful for discriminating wetland vegetation types (Brook & Kenkel, 2002); band 5 has been found particularly useful (Harvey & Hill, 2001; Johnston & Barson, 1993). Avoiding the use of the more haze-prone visible blue and green bands produced statistics less sensitive to within-scene atmospheric variability. The resistant z-score for each pixel on each scene was computed using

$$\tilde{z}_{ci} = \sum_{b=3}^{5} \frac{|x_{cbi} - \tilde{z}_{cb}|}{\tilde{\sigma}_{cb}} \quad (1)$$

where $\tilde{z}_{ci}$ is the resistant z-score of the ith pixel in class c; x_{cbi} is the band b reflectance of that pixel; $\tilde{x}_{cb}$ is the median band b reflectance of class c; and $\tilde{\sigma}_{cb}$ is the median absolute deviation of the band b reflectance of class c. Absolute values were used to maintain a strictly positive, non-directional total, and the orthogonal band z-scores were summed using the "city block" method (McCune & Grace, 2002) rather than the more typical Euclidean distance. The Euclidean distance, which utilizes the squares of the individual band scores, tends to weight the most atypical band more than the others. Because real land cover change should generally impact more than one of the TM bands, we felt that simple addition of the absolute-valued z-scores would be less susceptible to atmospheric noise and other errors in the sensor and data processing streams.

In order to provide indices more amenable to physical interpretation, resistant z-scores were also calculated on a tasseled cap transformation (TCT) of the spectral data. The TCT (Kauth & Thomas, 1976; Crist & Cicone 1984) provides the physically significant indices of "brightness," "greenness," and "wetness" (TC_b, TC_g, and TC_w) through a mathematical transformation of the spectral band reflectances. We calculated the TCT components for each scene using coefficients provided by Huang et al. (2002). Because we wanted to interpret change type through an examination of TCT z-scores, we omitted the absolute value from the

Table 1
Landsat scenes selected for use in this study

Path/Row	Spring date	Summer date	Fall dates
14/30	7 May 2001	23 Sep 1999	30 Oct 2001
14/31	5 Apr 2001	23 Sep 1999	30 Oct 2001
14/32	5 Apr 2001	23 Sep 1999	30 Oct 2001
14/33	5 Apr 2001	23 Sep 1999	25 Oct 1999
14/34	5 Apr 2001	23 Sep 1999	25 Oct 1999
14/35	5 Apr 2001	23 Sep 1999	25 Oct 1999
15/30	24 Mar 2000	2 Aug 2001	1 Nov 1999
15/31	24 Mar 2000	28 Jul 1999	1 Nov 1999
15/32	24 Mar 2000	28 Jul 1999	17 Nov 1999
15/33	24 Mar 2000	28 Jul 1999	9 Sep 1999
15/34	24 Mar 2000	28 Jul 1999	17 Nov 1999
16/30	19 Apr 2001	3 Jul 1999	13 Nov 2001
16/31	31 Mar 2000	4 Aug 1999	13 Nov 2001
16/32	31 Mar 2000	4 Aug 1999	13 Nov 2001
16/33	31 Mar 2000	4 Aug 1999	8 Nov 1999
16/34	31 Mar 2000	4 Aug 1999	8 Nov 1999
17/30	6 Mar 2000	12 Sep 1999	30 Oct 1999
17/31	6 Mar 2000	12 Sep 1999	30 Oct 1999
17/32	6 Mar 2000	12 Sep 1999	30 Oct 1999
17/33	6 Mar 2000	17 Sep 2001	30 Oct 1999
17/34	6 Mar 2000	10 Jun 2000	30 Oct 1999

Inter-scene variability in the dates selected for each season is acceptable, because z-scores are calculated on each scene independently and then merged. The spring date represents deciduous leaf-off conditions in all images, the summer represents leaf-on, and the fall dates vary but are generally consistent within each scene. Nearly all images were obtained by the Landsat 7 ETM+ sensor.

resistant *z*-score equation and instead computed a signed, directional *z*-score for each TCT component. The directional TCT resistant *z*-scores for each pixel on each scene were computed using

$$\tilde{z}_{\mathrm{TC}} = \tilde{z}_{c(\mathrm{b,g,w})i} = \frac{x_{c(\mathrm{b,g,w})i} - \tilde{x}_{c(\mathrm{b,g,w})}}{\tilde{\sigma}_{c(\mathrm{b,g,w})}} \quad (2)$$

where $\tilde{z}_{c(\mathrm{b,g,w})i}$ is the TC_b, TC_g, or TC_w resistant *z*-score of the *i*th pixel in class *c*; $x_{c(\mathrm{b,g,w})i}$ is the TC_b, TC_g, or TC_w of that pixel; $\tilde{x}_{c(\mathrm{b,g,w})}$ is the median TC_b, TC_g, or TC_w of class *c*; and $\tilde{\sigma}_{c(\mathrm{b,g,w})}$ is the median absolute deviation of the TC_b, TC_g, or TC_w of class *c*.

All computations were performed on a single TM scene at a time to avoid between-scene bias due to variations in atmospheric and hydrological conditions, and to reduce the geographic component of phenological and morphological vegetation variability within the wetland classes under analysis. However, analysis of single scenes reduced the number of pixels in each class available for computation of class statistics. If the number of available pixels for a particular class on a scene using the finest (238-class) aggregation was fewer than one hundred, the scores for pixels in that class were instead computed using the equivalent class in the finest higher level aggregation for which sufficient pixels were available. If fewer than one hundred pixels were available on the scene using even the coarsest (13-class) aggregation, no score was produced for pixels of that class on that scene. This procedure was repeated for all TM scenes in the study area, and for each of the three seasons of data. The individual scene scores were combined into seasonal mosaics by averaging scores produced in scene overlap areas. The seasonal mosaics were then combined by averaging the available scores across the three seasons.

2.5. Reference data

Reference data were needed to calibrate and validate the relationship between *z*-score and change probability. High quality digital orthophotos contemporary with the TM imagery were available from the states of New York, New Jersey, Delaware, West Virginia, and North Carolina. For a number of regions in these states, NWI provided us with the historic aerial photography used in their original mapping. This allowed us to determine whether wetlands appearing abnormal in recent photos had in fact changed and

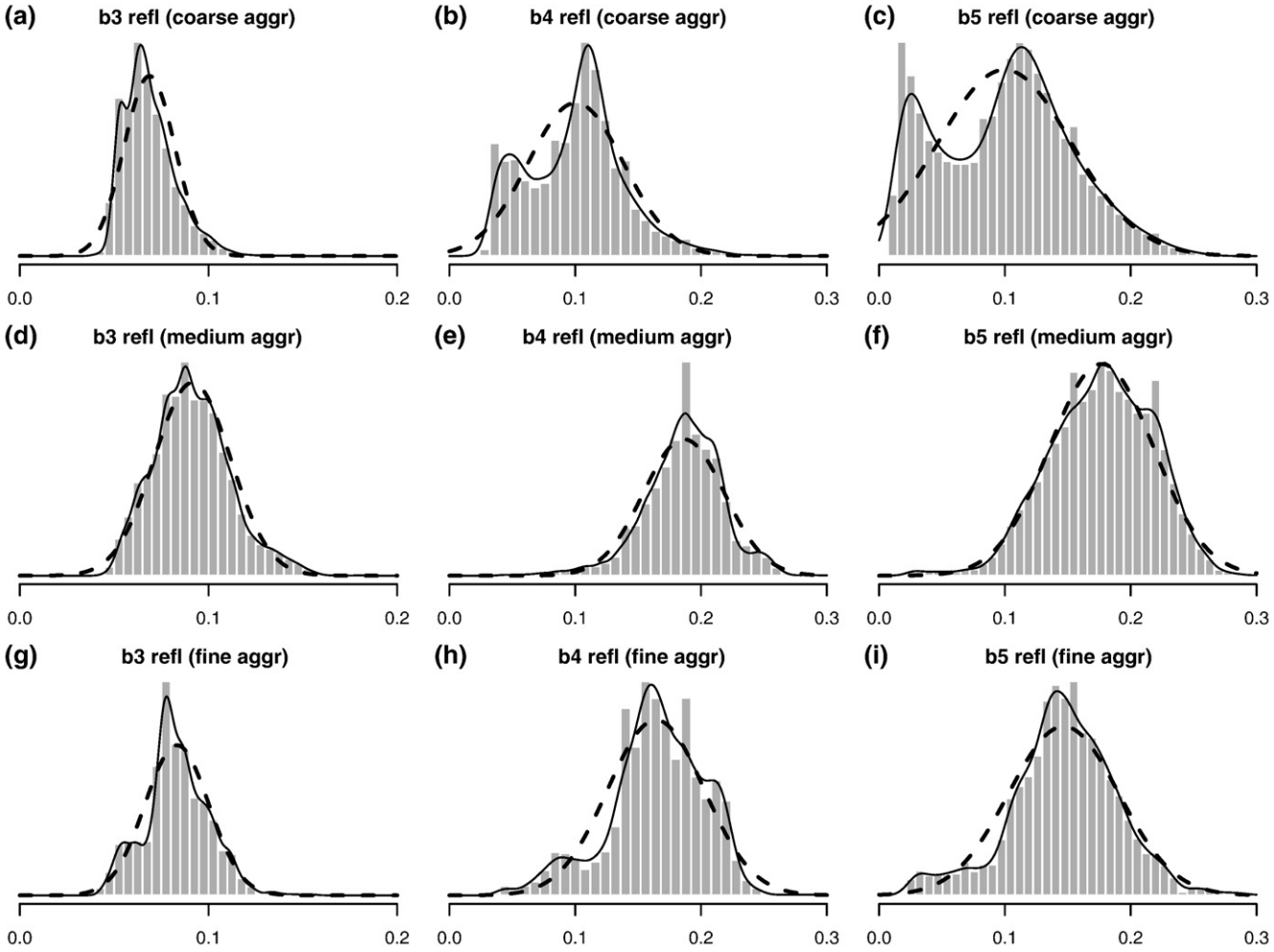

Fig. 3. Reflectance frequency histograms of TM bands 3 (red), 4 (near-IR), and 5 (mid-IR) at different levels of class aggregation for a springtime emergent wetland. The coarse aggregation (a–c) contains all emergent wetlands, the medium aggregation (d–f) contains only those that are non-tidal and seasonally wet, and the fine aggregation (g–i) additionally stipulates that the hydrological modifier be "seasonally flooded/saturated." Dashed lines represent normal approximations; effective use of RZA requires that histograms should be generally normal or log-normal. Bimodal distributions occur in the coarse aggregation due to the distinct reflectance characteristics of tidal and non-tidal wetlands.

Table 2
Wetland characteristics used to create the four aggregation levels, and the possible values associated with each

Characteristic	Possible values	Notes
Wetland system (used in all aggregation levels)	◦ Estuarine ◦ Palustrine	
Vegetation structure (used in all aggregation levels)	◦ Emergent ◦ Forest ◦ Shrub ◦ Other	
Vegetation phenology (used in all aggregation levels)	◦ Evergreen ◦ Deciduous ◦ Unknown	Including emergent vegetation persistent year-round Including non-persistent emergent vegetation Unspecified in NWI code
Hydrological regime (used in aggregation levels 1–3)	◦ Wet ◦ Tidal ◦ Seasonal ◦ Intermittent	Water typically covering surface Primarily influenced by tidal flooding Primarily influenced by seasonal flooding Typically not flooded
Mixed types (used in aggregation levels 1–2)		Structure and phenology of secondary vegetation types in mixed polygons maintained in levels 1 & 2; in higher levels only the primary type was kept.
Leaf geometry (used in aggregation level 1)	◦ Narrow ◦ Broad ◦ Unknown	Needle-leaved woody vegetation Broad-leaved woody vegetation Unspecified in NWI code
Hydrology (used in aggregation level 1)	◦ NWI modifiers	Retained wettest code specified

The coarsest level of aggregation (level 4) was based on only the first three characteristics and resulted in 13 wetland classes. The finest level (level 1), based on all characteristics shown, resulted in 238 classes.

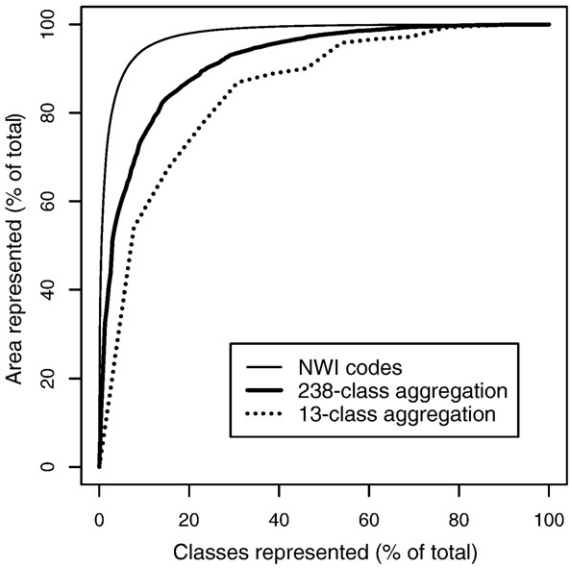

Fig. 4. Percent wetland area represented as a function of percent number of wetland classes included, for the coarsest and finest aggregation levels and the original NWI codes. Classes are added to the cumulative area function in descending order of size. The ideal aggregation strategy reflects a balance between the need for a large enough number of classes to represent variability and the need for classes sufficiently large to provide reliable statistics.

permitted a more certain assignment of change type. We made field visits to a few regions of intense wetland modification, further increasing confidence in our photointerpretation. Sample locations were randomly selected in areas covered by the historic photography, from populations stratified on the basis of wetland type, U.S. EPA ecoregion, and calculated *z*-score. Although we made an effort to represent the geographic range of the study area as well as possible within the constraints of the reference data, the large majority of samples were taken from the coastal plain between New Jersey and North Carolina.

In order to develop a stronger assessment of the methodology's change omission error rate, we gathered additional samples from each examined orthophoto by selecting wetlands showing visible change in the photography. Although this aspect of the sampling process was inherently non-random, we made an effort to select changed areas of a variety of types and sizes. A total of 277 sample areas – 156 from the stratified random sampling, and the remainder visually selected to test omission error – were photointerpreted to ascertain a range of characteristics descriptive of their conditions at the time of NWI mapping and circa year 2000, including, but not limited to, land use and land cover, change type (if any), and degree of heterogeneity. The interpreted areas were approximately 1 ha in size, centered on the randomly selected point.

Many types of change were observed and interpreted; if multiple types were encountered, that causing the most intense change in land surface conditions was recorded. Many of the change type interpretations (e.g., where land clearance had occurred but no construction had yet taken place) relied on assessing the spatial context within which the change occurred. Before conducting statistical analysis, we recoded photointerpreted change types to a simple variable representing major change, minor change, or no change. For this purpose, major change was defined as change that resulted in nearly complete vegetation removal, exposure or disturbance of soil, or a large change in the proportion of the ground surface covered by water. Minor change represented all other changes detectable in aerial photography. Occasionally it proved impossible to determine whether

Table 3
Change types used in photointerpretation process, the change category to which they belong, their descriptions, and the intensity of change they were recoded to for validation purposes

Change category	Change type description	Intensity
Development	◦ Converted to extractive (e.g., mining) purposes	Major
	◦ Developed for residential or commercial use	Major
	◦ Developed for farm/rural use	Major
	◦ Road construction	Major
Land clearance	◦ Land cleared for residential or commercial development	Major
	◦ Land cleared for agricultural development, including logging where forest regeneration unlikely	Major
	◦ Land cleared and converted to plantation forestry	Major
	◦ Land cleared for development other than agriculture or urban use	Major
	◦ Land cleared, bare soil exposed; purpose uncertain	Major
Logging	◦ Logged and converted to plantation forestry	Major
	◦ Forest with over 50% of canopy vegetation removed	Minor
	◦ Logged; less than 50% of canopy vegetation removed	Minor
Vegetation modification	◦ Vegetation removed by flooding, insect damage, etc.	Major
	◦ Altered, but not extensively, by flooding, insect damage, etc.	Minor
	◦ Shift in physiognomic type due to natural succession	Minor
	◦ Shift in physiognomic type for any reason	Minor
Hydrologic modification	◦ Naturally unflooded area now mostly flooded; little live vegetation visible during growing season	Major
	◦ Amount of surface water increased substantially	Minor
	◦ Decrease in amount of standing water or soil water content; often as consequence of wetland drainage	Minor
Recovery	◦ Formerly drained area had natural hydrology restored	Minor
	◦ Formerly flooded area no longer flooded (e.g., dam removal)	Minor
Other	◦ No change observed	None
	◦ Apparent misinterpretation or coding error in NWI data	None
	◦ Unknown	Unknown

change had occurred or not; these samples were discarded. The change type descriptions and their coding as major or minor change are shown in Table 3.

We also compared the RZA results with two other sources of spatially explicit reference data that overlapped the study area. Erwin et al. (2004) used a time series of aerial photography to map marsh loss through 1994 on the eastern shore of Virginia, and provided us with a digital representation of their results. RZA change predictions were also visually compared to published maps of similar marsh loss in Jamaica Bay, New York (Hartig et al., 2002).

2.6. Change probability calibration

We used a binomial logistic regression in order to calibrate the relationship between *z*-score and change probability. In order to implement this, we needed to first collapse the plot change data to a binary change/no-change indicator. After verifying that requirements of normality were met, we assessed the degree of separability of major change, minor change, and no-change plots by examining the *z*-score histograms of the three groups and by using an ANOVA procedure to determine whether the minor change plots would be more effectively treated as change or no change for the purpose of binomial modeling. We recoded the change data based on the outcome of this test, and then performed a logistic regression of binomial change data against *z*-score. For this purpose we used only the plot data that had been randomly selected.

We performed a number of statistical tests in order to assess the appropriateness of the logistic model and the strength of the modeled relationship. We performed a model χ^2 test on the difference between the residual and null deviances to evaluate the null hypothesis of no linear relationship between *z*-score and the natural log of the odds of change, and calculated D^2 and Nagelkerke's R^2, measures which estimate the proportion of variability explained by the model and represent logistic equivalents to the R^2 coefficient of determination. We then applied a χ^2 test to evaluate the significance of the error remaining in the model after incorporation of *z*-score. Finally, in order to test the fit of the logistic model to the data, we performed a χ^2 "goodness of fit" test between binned observations and expected values and produced a calibration plot showing the 95% confidence interval of the proportion of plots changed in each bin.

2.7. Accuracy assessment

After evaluating the fit of the developed logistic model, we applied the model to all our reference data, including the targeted change

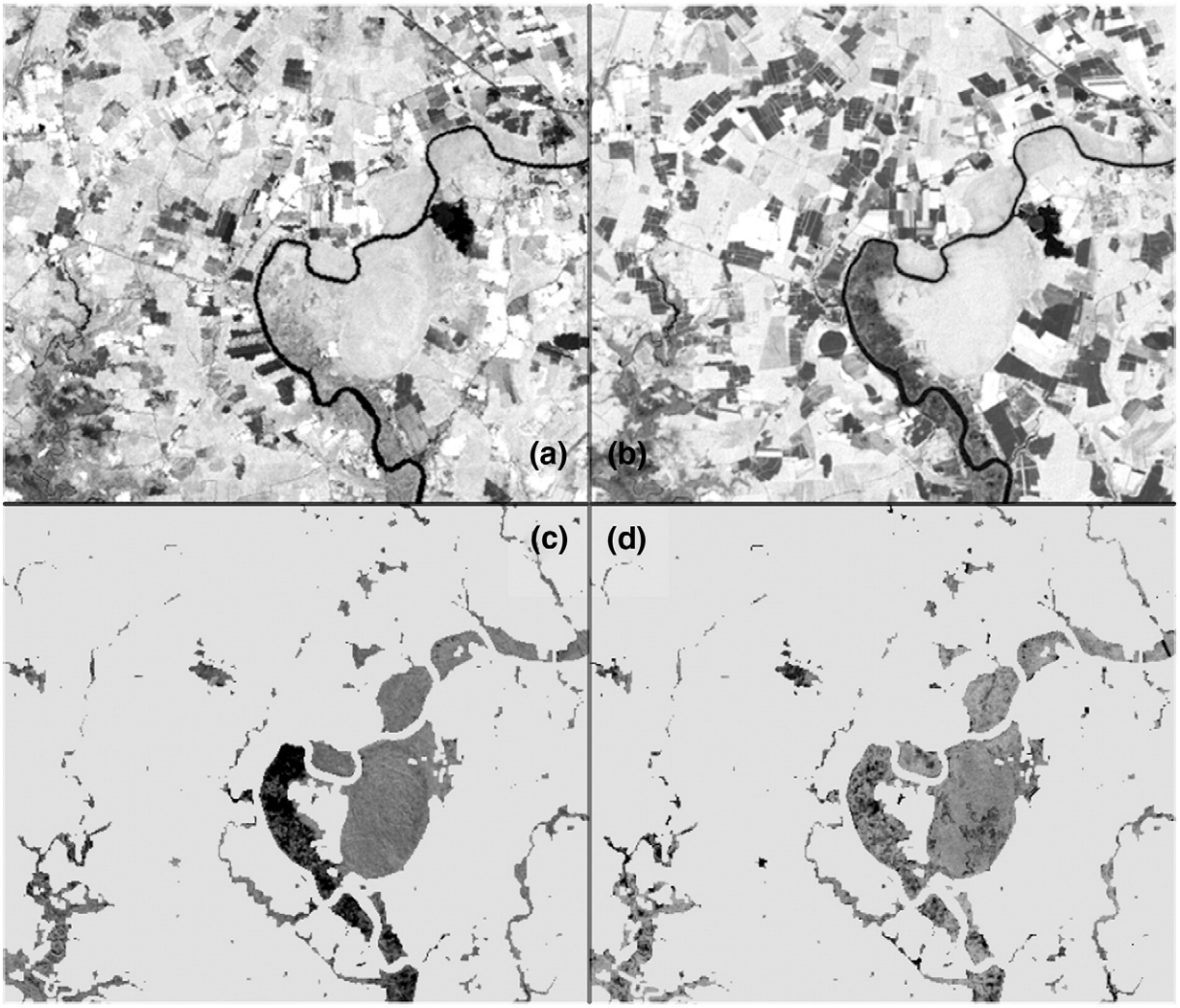

Fig. 5. The upper two images show mid-summer NDVI for an area of coastal Maryland in 1990 (a) and 1999 (b). Conventional image differencing (the sum of the absolute differences in bands 3, 4, and 5) produced the results in (c), where darker shades represent increasing change intensities. Tidal stage variation along the river caused high change probabilities in emergent floodplain vegetation. RZA (d) is less sensitive to tidal stage because the entire classes of analysis pixels are similarly impacted, allowing real change to be more easily identified.

plots, and plotted Cohen's κ, a measure of the model's improvement over random predictions, across the range of possible threshold values. We also produced a Receiver Operating Characteristic (ROC) curve, a threshold-independent metric to evaluate the model's overall sensitivity and false alarm rate. Finally, in order to assess the generality of the model developed, we split all the reference data randomly into two sets and generated an optimum threshold using the first set. We then assessed the accuracy of predictions made using the threshold against the second, independent data set by generating a confusion matrix and calculating Cohen's κ.

3. Results

3.1. Identification of change under conditions of natural variability

Fig. 5 illustrates the differences in results between conventional image differencing and RZA, as applied to an area on the eastern shore of Maryland. Tidal emergent wetlands along a river are flagged as changed by the image difference because the more recent image was obtained during a higher tidal stage than the historic image. RZA change detection is far less sensitive to this problem because most wetlands of that analysis class are inundated, causing the expectation for the class to reflect the flooded state.

Visual comparisons of RZA change estimates to the fine-scale. Erwin et al. (2004) and Hartig et al. (2002) reference data yielded favorable results, assuming proper calibration of the relationship between z-score and change likelihood. Marsh loss polygons delineated by Erwin et al. (2004) are shown in Fig. 6 against a backdrop formed by the z-scores derived from RZA. The correspondence is good, despite the fact that some polygons are not much wider than a TM pixel. The area of high z-scores indicated by the arrow appears in aerial photography to be an area of sediment buildup; Erwin et al. (2004) mapped only flooded wetlands and so omitted this area. Directional z-scores based on TCT components can distinguish and map both phenomena separately. RZA change estimates also showed a high degree of agreement with the Jamaica Bay marsh loss maps of Hartig et al. (2002; not shown).

3.2. Separability assessment

The resistant z-score frequency histograms for the major change, minor change, and no-change codes are shown in Fig. 7. A one-way ANOVA means test performed on the randomly sampled portion of the reference data indicated that the means of the three change codes were not equal ($p \ll 0.001$). In order to determine the best grouping of the three change codes into a binomial classification, a Tukey test (Zar, 1996) was run to test the significance of differences in mean between (a) the no-change code and the combined minor and major change codes, and (b) the major change code and the combined no change and minor change codes. Both groupings showed equally significant differences in means ($p \ll 0.001$). Since using grouping (a) would produce a more sensitive model, we chose to lump the minor and major change codes and to parameterize the logistic regression to simply distinguish changed from unchanged wetlands.

3.3. Logistic regression

The logistic model found a strong relationship between z-score and change probability, based on the 156 randomly selected change/no-change sample points from which it was built (Table 4). The model χ^2 test rejected the null hypothesis of no linear relationship between z-score and the log-odds of wetland change ($p \ll 0.001$). D^2 and Nagelkerke's R^2 were found to be 0.473 and 0.633, respectively. The model residual deviance was non-significant ($p = 0.998$). The data were binned into eight groups in order to run the χ^2 goodness of fit test; in order to meet the rule of thumb that no bins should have model expectations of less than one (Zar, 1996) we eliminated data from the extreme low and high tails of the z-score distribution. The dropped data were well-modeled and removing them should not have affected the conclusions. The test resulted in an acceptance of the null hypothesis that there was no difference between observed and model-estimated values and that the logistic model is appropriate for the data ($p = 0.315$). A calibration plot illustrating the 95% confidence intervals for each bin is shown in Fig. 8; all intervals overlapped the 1:1 line of perfect change probability estimation.

3.4. Accuracy assessment

The ROC curve and accuracy measures against the range of possible threshold values for all reference data are shown in Fig. 9. The optimal κ, at a threshold of $p_{\text{change}} = 0.2925$, was 0.817, indicating a strong improvement over randomness. The area under the ROC curve of 0.94 (out of a possible maximum of 1.0) also signified a well-fitted model, with high sensitivity and resistance to false alarms. The optimal

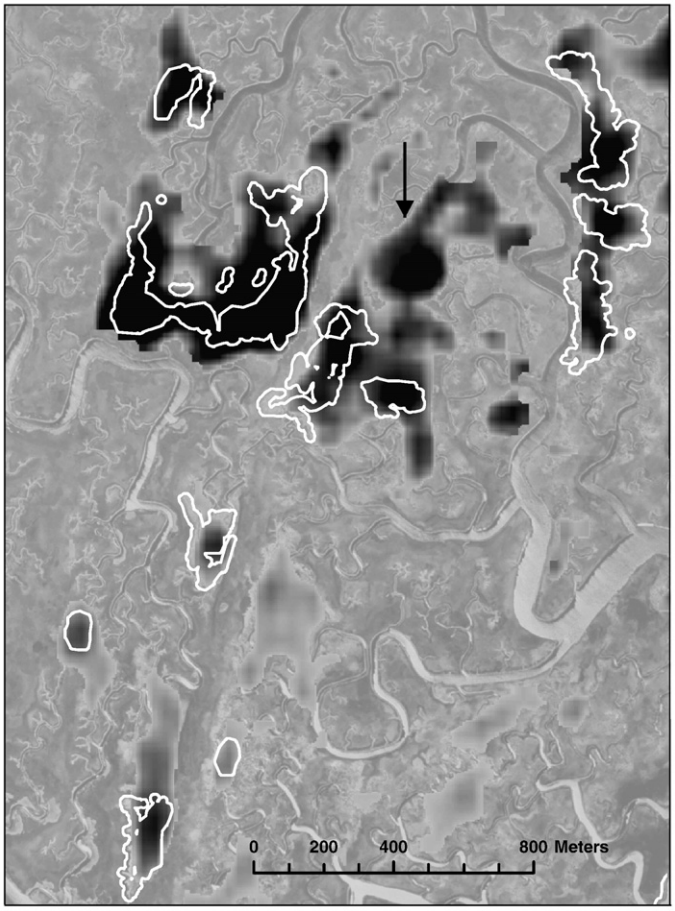

Fig. 6. White-outlined polygons represent areas of coastal marsh loss to tidal ponds and open water on Virginia's eastern shore (Erwin et al., 2004, buffered slightly here to remove excessive detail). Dark shaded areas represent high RZA wetland change likelihood circa year 2000, spatially smoothed to higher resolution for better comparison with the polygons. The RZA change area indicated by the arrow appears in aerial photography to be an area of sediment accumulation rather than flooding and thus was not mapped by Erwin et al. Other inconsistencies may be due to changes that occurred between 1994 and 2000.

threshold generated from the randomly selected training data set, p_{change}=0.295, was nearly identical to that generated from all reference data. The confusion matrix derived from the application of this threshold to the independent validation data is shown in Table 5, and resulted in a κ of 0.779, an overall prediction accuracy of 89.5%, and low rates of both commission and omission errors.

3.5. Change probability mapping

The logistic equation relating resistant *z*-score to change probability was applied to all pixels across the study area, producing a comprehensive map of the probability of wetland change since the date of NWI mapping in the 1970s and 1980s. We produced an estimate of local change intensity – the proportion of wetland area changed – by spatially aggregating pixel change probabilities. In order to visualize small patches of wetland change and areas of moderate change intensity more easily over large spatial extents, we averaged pixel change probabilities at scales of 500 to 1500 m, and used a logarithmic color ramp. Wetland change intensity from the date of NWI base mapping to approximately year 2000 is shown for a large portion of the study area in Fig. 10. Major hotspots of wetland change were found in the coastal areas of southern Virginia and northern North Carolina, where many forested wetlands have been converted to agriculture and residential development, and in regions of salt marsh loss bordering the Chesapeake and Delaware Bays. Many smaller discrete areas of change were found, primarily concentrated near population centers.

4. Additional applications

Brief accounts of two additional applications for which we have used the RZA techniques are given here. We hope these will encourage natural resource scientists and land managers to consider use of this or related remote sensing-based techniques for their own application needs.

4.1. Regional monitoring of marsh degradation

Relative sea level rise is occurring along the coastlines of the eastern U.S. and is causing the loss of salt water marshes, particularly on the Gulf coast and the mid-Atlantic seaboard (Morris et al., 2002; Hartig et al., 2002; Erwin et al., 2004). This concern has been addressed via remote sensing by applying spectral mixture modeling to TM imagery to estimate the fraction of each pixel occupied by water (Kearney et al., 2002; Rogers & Kearney, 2004). However, spectral

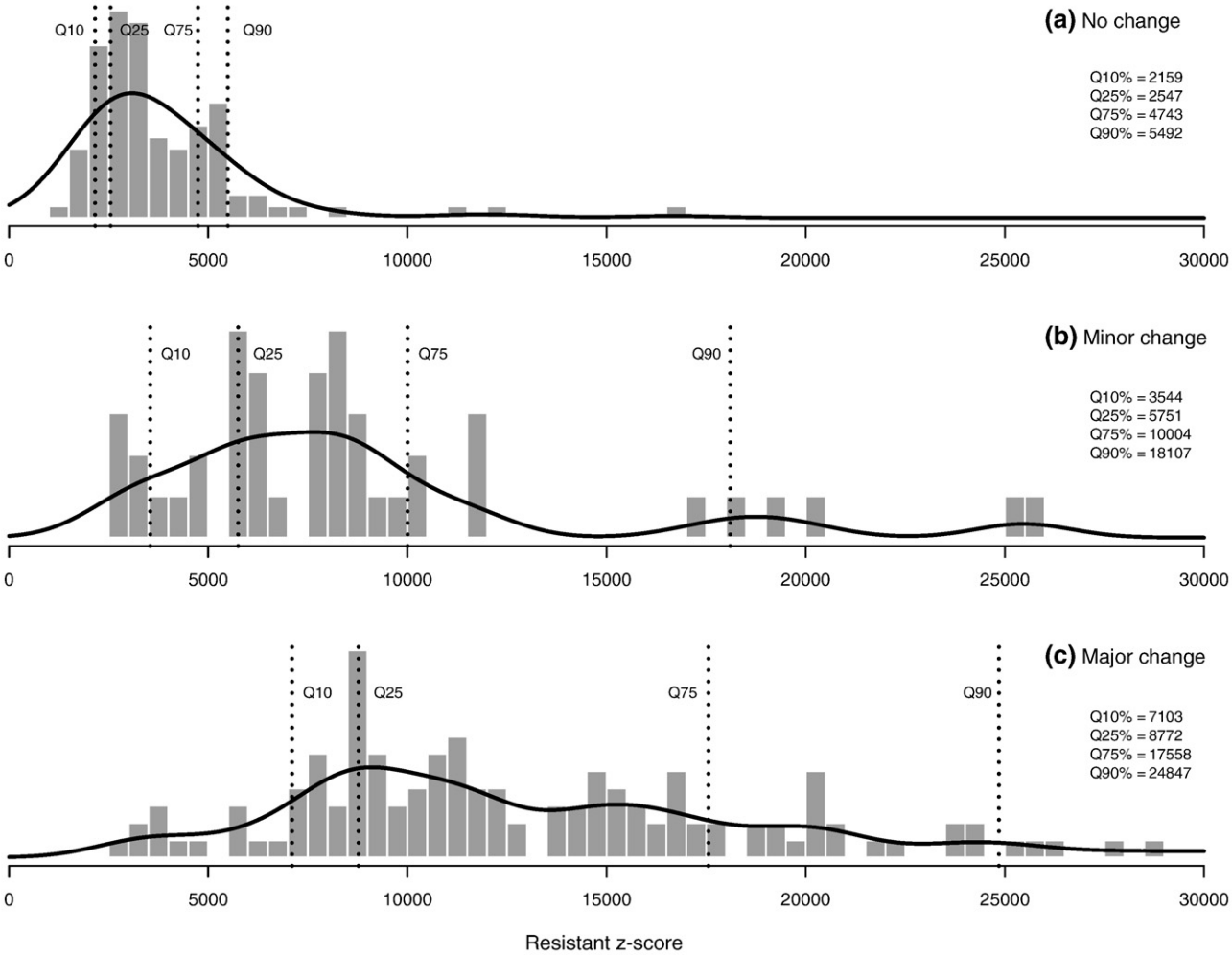

Fig. 7. Resistant *z*-score histograms of sampled no change, minor change, and major change areas. A smoothed kernel density estimate and the 10%, 25%, 75%, and 90% quantiles are shown for each change category. Both major and minor change are reasonably separable from no change: $Q75_{no\ change} < Q25_{minor\ change}$ indicates a fair ability to distinguish minor change, while $Q90_{no\ change} < Q10_{major\ change}$ indicates that major change can be clearly discriminated.

mixture modeling is a complex process relying on accurate parameterization and is highly sensitive to between-scene changes in vegetation phenology and tidal and atmospheric conditions. Consequently, consistent application over multi-scene areas is challenging. In addition, the output is a measure of current inundation across the landscape without reference to former conditions, which may not be ideal for assessing change.

RZA can be used to circumvent some of these difficulties. When marshes are lost, decreases in summer TC_g can be expected, as well as increases in TC_w for all seasons. We therefore represented coastal marsh inundation with an index formed by subtracting the summer TC_g resistant z-score from the averaged spring and summer TC_w scores. The resulting index has its highest values for pixels with above normal TC_w and below normal TC_g, and so can be used to quantify marsh degradation. Because this index is determined on a per-class basis, it represents inundation relative to prior conditions and thus reflects change rather than simply current conditions. Quantitative use of the index would require calibration for the task being addressed, which was not done here. However, the relative values of the index are useful for interpretation purposes. Fig. 11 shows the relative degree of marsh degradation estimated for an area on the eastern shore of the Chesapeake Bay which includes Blackwater National Wildlife Refuge, where marsh loss has been severe (Kearney et al., 2002).

4.2. Invasive species mapping

An invasive variety of the reed grass *Phragmites australis* has spread widely in tidal marshes along the mid-Atlantic coast (Leonard et al., 2002). Our research has indicated that the morphological and stand structure of this plant cause much higher TC_g and TC_b z-scores than are associated with the native marsh vegetation. The Nature Conservancy mapped the distribution of the plant along the Virginia eastern shore in 1996 using aerial videography (Ngu et al., 1996). The patches they delineated are shown superimposed on year 2000 TC_b scores in Fig. 12. Research by Thomas (2006) lent additional support to the mapping of *Phragmites* using RZA, but found that the TC_w score is the strongest indicator of its presence.

5. Discussion

5.1. Assessment of resistant z-score analysis for wetland change monitoring

Based on the performance of RZA in detecting change in the test data, we conclude that it can successfully identify potential locations and hotspots of wetland change. In general, these areas are worthy of further investigation at a finer spatial scale and with more attention to individual site characteristics. However, although RZA performed well in the tests here, there are several reasons to be cautious in interpreting the results.

The extreme natural variability of wetlands and the spatial heterogeneity of the processes which impact them can cause problems that are difficult to circumvent without more sophisticated modeling. For instance, our map indicated a high likelihood of change in a number of wetland areas along the Passaic River in northern New Jersey. These wetlands were flooded when the spring TM image was collected for this area, a natural occurrence there at that time of year. Although RZA compared the Passaic wetlands only to others classified similarly by NWI, most other wetlands of that class were not flooded, whether due to differing hydrological characteristics or spatial variability in storm or snowmelt patterns. Consequently, a high z-score for the Passaic wetlands was calculated in the spring image and propagated at a reduced strength through the subsequent seasonal averaging process. Tidal movement time lags could create similar challenges, particularly in large estuaries such as the Chesapeake Bay (Kearney et al., 2002). Although RZA is less impacted by tidal variation than simple image differencing, inconsistencies due to spatial variability in tidal timing may not be easily resolved.

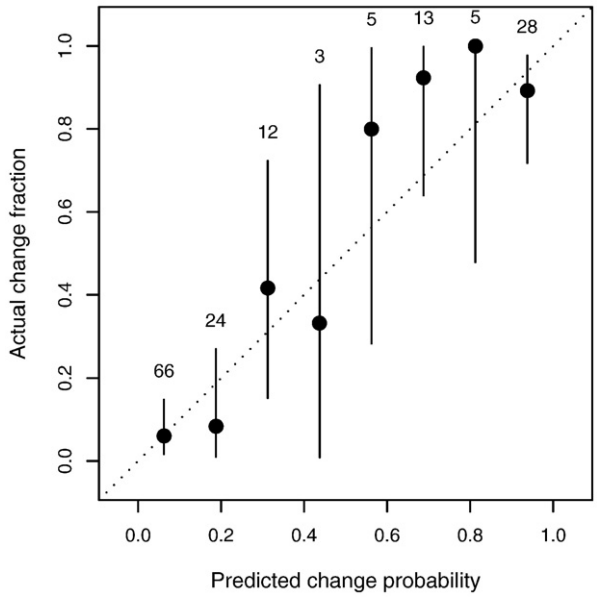

Fig. 8. Sample plot change fraction for binned change probability intervals vs. mean bin change probability, with 95% confidence intervals. The number of sample plots falling in each bin appears above the confidence interval bars. All sample plots used here were randomly selected, stratified on resistant z-score. The 1:1 line representing a perfect logistic fit is shown; all confidence intervals overlap it. Figure produced using routines from Freeman (2007).

Table 4
Assessment of logistic model for prediction of change probability from resistant z-score

Test	Chi square	*df*	*P*
Null deviance	205.89	155	0.004
Residual deviance	108.54	154	0.998
Model χ^2	97.35	1	$\ll$0.001
Goodness of fit	7.063	6	0.315
D2 = 0.473			
Nagelkerke's R^2 = 0.633	$\ln\left(\frac{p_{chg}}{1-p_{chg}}\right) = -4.296 + 0.000615 \cdot \tilde{z}$		

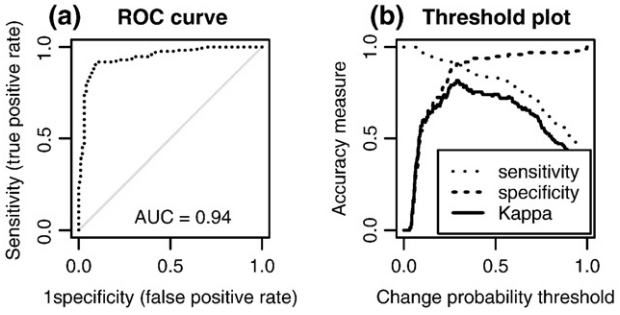

Fig. 9. Image (a) is the ROC curve for the logistic regression, calculated based on all sample data. The optimal probability classification threshold based on minimization of the curve distance from the upper left origin is 0.29. The area under the curve (0.94) signifies a well-fit model. Image (b) is a plot of several accuracy measures against change probability threshold. The threshold based on optimizing Kappa is identical to that based on minimizing ROC curve distance. Figure produced using routines from Freeman (2007).

Table 5
Accuracy assessment of wetland change prediction based on thresholded change probability, evaluated against independent validation data

Predicted	Observed		
	Change	No change	Percent correct
Change	76	5	93.8%
No change	9	44	83.0%
Percent correct	89.4%	89.8%	
Commission error	6.17%	Overall accuracy	89.6%
Omission error	10.6%	Cohen's κ	0.779

Silvicultural activities are another major source of confusion, particularly if the goal of the analysis is to detect wetland loss rather than simply land cover change. Much of the forested land in the coastal portion of the study area – including some wetlands – is occupied by loblolly pine plantations, which are characterized by a short rotation time, clearcutting, and subsequent replanting. Drastic changes in reflectance are therefore a common feature of the landscape in this area. These changes are not associated with wetland loss, although they cause change in vegetation structure and potential degradation of some of the wetland functionality discussed above. Similarly, some land use changes, such as introduction of livestock grazing, may have large impacts on reflectance characteristics while allowing the continued existence of wetlands. Such ambiguities would manifest themselves as variation in the relationship between *z*-score and change probability, depending on wetland type and the change process undergone. A cautious interpretation of indicated change in our current map product is therefore essential.

5.2. Prospects for further development

Although we have not yet evaluated the magnitude of the above factors' influence on the relationship between *z*-score and change

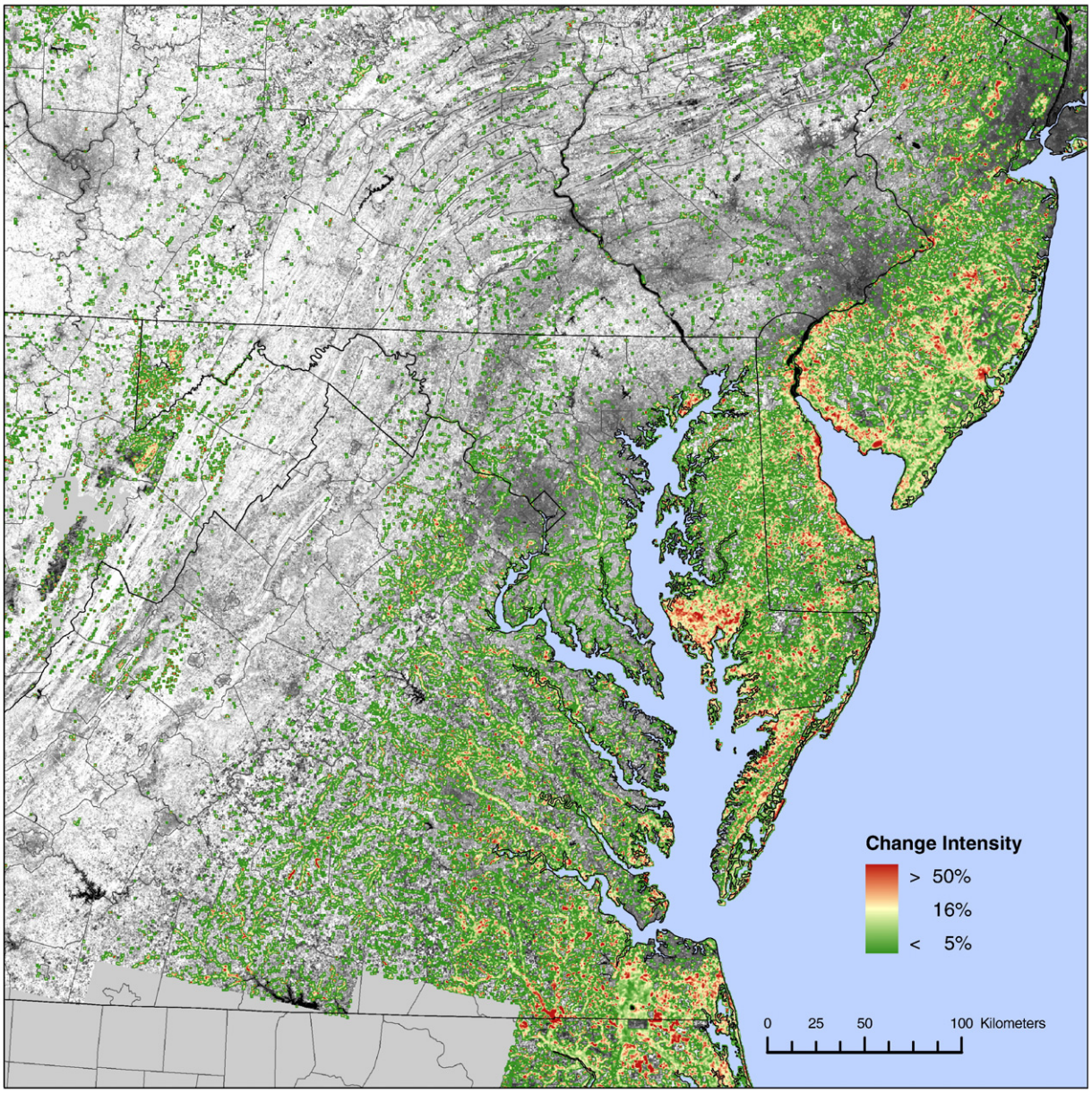

Fig. 10. Estimated change intensity across a large part of the study area. The beginning of the time period over which change is estimated is determined by the date of NWI base mapping, and so varies across the study area, but is generally from the late 1970s to early 1980s. The end of the change estimation time period is approximately year 2000.

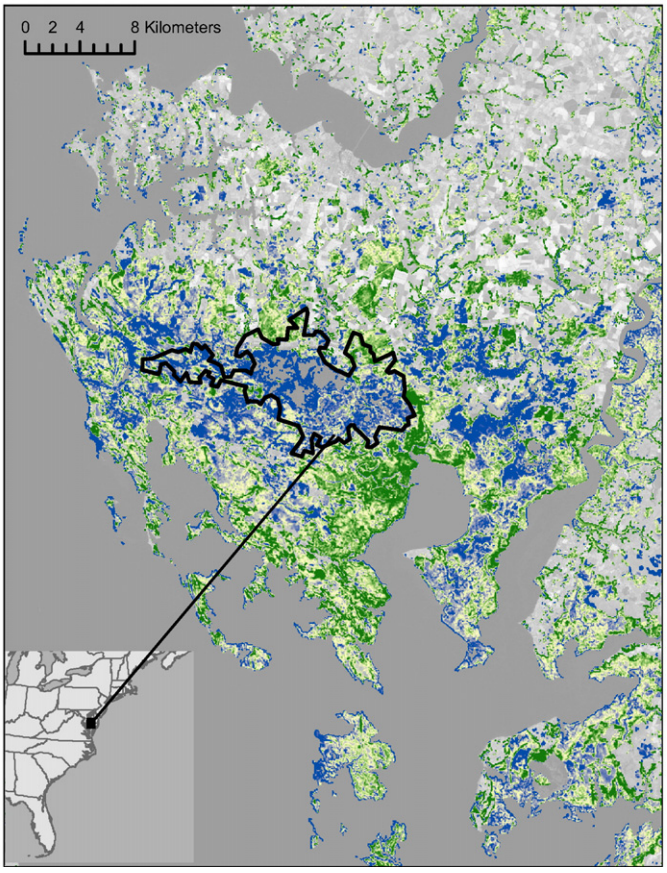

Fig. 11. RZA-estimated coastal marsh degradation in the area of Blackwater National Wildlife Refuge on the Chesapeake Bay in eastern Maryland. Green areas represent relatively intact marsh, with yellow and blue representing increasing likelihood and intensity of degradation and conversion to open water. The wildlife refuge is represented by the black polygon; uncolored areas within it were mapped as open water by NWI.

probability, it is likely that calibrating the logistic regression to produce an equally reliable and unbiased change probability for all wetland types and change processes would require a substantial increase in sampling intensity. An increase in the amount of reference data would also permit the construction of a multiple logistic regression based, perhaps, on the seasonal directional TCT *z*-scores, which would place greater weight on key diagnostic features for detecting change in different wetland environments. If change type is found to strongly influence the *z*-score/change probability relationship, it would be necessary to construct a decision-making procedure by which the change process most likely to be operating on any pixel could be identified. That information could then drive a logistic regression parameterized for change type. Directional TCT *z*-scores and local land use information would probably play a major role in any determination of change type.

Change probabilities could be aggregated over summary areas such as counties and watersheds for comparative purposes. However, potential biases due to the influence of wetland and change type on the change probability relationship would first need to be addressed. Otherwise, change rates in areas dominated by some wetland or land use types (e.g., plantation forestry) would not be comparable to those in other areas. Domination of some areas by problematic wetland types (e.g., narrow riparian wetlands or fringing wetlands that are difficult to resolve at 30-meter resolution) would likewise cause problems of comparability. In addition, the variable baseline date of the NWI maps causes the change detection time period to differ between areas. Fully automated updating of NWI maps would encounter the same problems, along with additional difficulties such as the spatial ambiguities of NWI mixed polygons, in which a polygon is composed of two distinct wetland types but no spatial information is provided as to where each is located.

Outlier detection is ultimately limited by the quality and consistency of the original map product. While the NWI data are remarkable considering the magnitude of the task they address, omissions and misclassifications will occasionally be encountered. Omitted and newly created wetlands cannot be addressed by this methodology. RZA is by no means a method of improving the baseline maps upon which it is run, but rather provides a tool to identify land cover changes and make revisions and pattern assessments in the absence of a comprehensive repetition of the process by which the baseline maps were originally made.

6. Summary and conclusions

It is difficult to confidently detect change in land cover types that exhibit high temporal rates of natural variability, particularly if that variability occurs unpredictably or varies in amplitude. Wetlands are an excellent example,[2] since water moves in and through the systems at rates that vary at several temporal scales and in response to other variables (e.g., precipitation). However, by using outlier-resistant statistical estimators and appropriate aggregations of NWI wetland classes, RZA allows the computation of a relatively consistent measure of wetland change probability. We used this measure to produce a regional map of change probability for the mid-Atlantic region. The method avoids the difficulties of atmospheric and phenological variability inherent in change detection based on image differencing. The resulting map can be used to target areas for closer inspection and investigation on a site-specific basis, and the technique has a number of other potential specific applications at both regional and local scales. With additional work to resolve confusion resulting from natural spatial heterogeneity and land use patterns, this technique could form the core of a process to produce updates to NWI maps, and to compute wetland change rates on an areal basis. Three conditions are necessary in order to employ RZA for these applications. The most basic applications require that (1) change rates are not so high as to cause the statistical measures to be non-representative of unchanged wetlands; and (2) unchanged classes exhibit somewhat normal or at least unimodal reflectance distributions. Map updates and areal change rate determination require that (3) the relationship between reflectance atypicality and change probability can be parameterized across wetland types, geographic regions, and land use categories.

Acknowledgements

This work was partly supported by the U.S. EPA Chesapeake Bay Program, George Mason University, and the NASA-Goddard Space Flight Center. The staff at the NWI office in St. Petersburg, Florida, particularly Kim Santos, helped us immensely by locating and sharing vintage NWI aerial photography. Statistical analysis was done primarily using R (http://www.R-project.org), and particular use was made of the PresenceAbsence package, developed by Elizabeth Freeman of the U.S. Forest Service Rocky Mountain Research Station in Ogden, Utah. Some data used in this publication were provided by the Virginia Coast Reserve LTER project, supported by National Science Foundation grants BSR-8702333-06, DEB-9211772, DEB-9411974 and DEB-008038. Special thanks to

[2] Agricultural systems – particularly crops – are another variable land cover type in which RZA change detection would likely be helpful.

Fig. 12. *Phragmites australis* patches mapped through aerial videography by Ngu et al. (1996) are represented by white polygons. They are superimposed on 3-season averaged TC_b resistant *z*-scores in which dark shaded areas represent areas of abnormally high brightness in the year 2000. The plant may have continued to spread in the time between the aerial assessment and the TM imagery used here.

Nancy Thomas of the University of Maryland for many helpful discussions.

References

Brinson, M. M., & Malvarez, A. I. (2002). Temperate freshwater wetlands: Types, status, and threats. *Environmental Conservation*, *29*, 115–133.

Brook, R. K., & Kenkel, N. C. (2002). A multivariate approach to vegetation mapping of Manitoba's Hudson Bay Lowlands. *International Journal of Remote Sensing*, *23*, 4761–4776.

Cowardin, L. M., Carter, V., Golet, F. C., & LaRoe, E. T. (1979). *Classification of wetlands and deepwater habitats of the United StatesFWS/OBS-79/31.* (pp.) Washington, DC: U.S. Department of Interior, Fish and Wildlife Service 79 pp.

Crist, E. P., & Cicone, R. C. (1984). A physically-based transformation of Thematic Mapper data: The TM tasseled cap. *IEEE Transactions on Geoscience and Remote Sensing*, *22*, 256–263.

Dahl, T. E. (2006). *Status and trends of wetlands in the conterminous United States 1998 to 2004.*Washington, DC: U.S. Department of Interior, Fish and Wildlife Service 112 pp.

Dobson, J. E., Bright, E. A., Ferguson, R. L., Field, D. W., Wood, L. L., Haddad, K. D., et al. (1995). NOAA Coastal Change Analysis Program (C-CAP): Guidance for regional implementation. *NOAA technical report NMFS, 123* Washington, DC: U.S. Dept. of Commerce 92 pp.

Erwin, R. M., Sanders, G. M., & Prosser, D. J. (2004). Changes in lagoonal marsh morphology at selected northeastern Atlantic coast sites of significance to migratory waterbirds. *Wetlands*, *24*, 891–903.

Freeman, E. (2007). *The presenceabsence package, version 1.0.0.* Online: http://cran.r-project.org

Gibbs, J. P. (2000). Wetland loss and biodiversity conservation. *Conservation Biology*, *14*, 314–317.

Hansen, M., DeFries, R. S., Townshend, J. R. G., Sohlberg, R., Dimiceli, C., & Carroll, M. (2002). Towards an operational MODIS continuous field of percent tree cover algorithm: Examples using AVHRR and MODIS data. *Remote Sensing of Environment*, *83*, 303–319.

Hartig, E. K., Gornitz, V., Kolker, A., Mushacke, F., & Fallon, D. (2002). Anthropogenic and climate-change impacts on salt marshes of Jamaica Bay, New York City. *Wetlands*, *22*, 71–89.

Harvey, K. R., & Hill, G. J. E. (2001). Vegetation mapping of a tropical freshwater swamp in the Northern Territory, Australia: A comparison of aerial photography, Landsat TM and SPOT satellite imagery. *International Journal of Remote Sensing*, *22*, 2911–2925.

Houhoulis, P. F., & Michener, W. K. (2000). Detecting wetland change: A rule-based approach using NWI and SPOT-XS data. *Photogrammetric Engineering and Remote Sensing*, *66*, 205–211.

Huang, C., Wylie, B., Yang, L., Homer, C., & Zylstra, G. (2002). *Derivation of a tasseled cap transformation based on Landsat 7 at-satellite reflectance.* Sioux Falls, SD: USGS EROS Data Center.

Jain, A., Nandakumar, K., & Ross, A. (2005). Score normalization in multimodal biometric systems. *Pattern Recognition*, *38*, 2270–2285.

Johnston, R. M., & Barson, M. M. (1993). Remote sensing of Australian wetlands: An evaluation of Landsat TM data for inventory and classification. *Australian Journal of Marine and Freshwater Research*, *44*, 235–252.

Kauth, R. J., & Thomas, G. S. (1976). The tasseled cap: A graphic description of the spectral-temporal development of agricultural crops as seen by Landsat. *Final proceedings: Second international symposium on machine processing of remotely sensed data* (pp. 41–51). West Lafayette, IN: Purdue University.

Kearney, M. S., Rogers, A. S., Townshend, J. R. G., Rizzo, E., Stutzer, D., Stevenson, J. C., et al. (2002). Landsat imagery shows decline of coastal marshes in Chesapeake and Delaware Bays. *Eos Transactions of the American Geophysical Union*, *83*, 173–178.

Kennish, M. J. (2002). Environmental threats and environmental future of estuaries. *Environmental Conservation*, *29*, 78–107.

Koeln, G., & Bissonnette, J. (2000). Cross-correlation analysis: Mapping landcover change with a historic landcover database and a recent, single-date multispectral image. *Proceedings of the 2000 ASPRS Annual Convention* 8 pp.

Koneff, M. D., & Royle, J. A. (2004). Modeling wetland change along the United States Atlantic coast. *Ecological Modelling*, *177*, 41–59.

Kudray, G. M., & Gale, M. R. (2000). Evaluation of National Wetland Inventory maps in a heavily forested region in the upper Great Lakes. *Wetlands*, *20*, 581–587.

Leonard, L. A., Wren, P. A., & Beavers, R. L. (2002). Flow dynamics and sedimentation in *Spartina alterniflora* and *Phragmites australis* marshes of the Chesapeake Bay. *Wetlands*, *22*, 415–424.

Lu, D., Mausel, P., Brondízio, E., & Moran, E. (2004). Change detection techniques. *International Journal of Remote Sensing*, *25*, 2365–2407.

Lunetta, R. S., & Balogh, M. E. (1999). Application of multi-temporal Landsat 5 TM imagery for wetland identification. *Photogrammetric Engineering and Remote Sensing*, *65*, 1303–1310.

McCune, B., & Grace, J. B. (2002). *Analysis of ecological communities.*Gleneden Beach, OR: MjM Software Design 300 pp.

Morris, J. T., Sundareshwar, P. V., Nietch, C. T., Kjerfve, B., & Cahoon, D. R. (2002). Responses of coastal wetlands to rising sea level. *Ecology*, *83*, 2869–2877.

Ngu, D., Albertson, J. D., Blum, L. K., & Truitt, B. (1996). Phragmites distribution in 1996 on the eastern shore of Virginia. *Virginia Coast Reserve Long Term Ecological Research Dataset, VCR01070* Online: http://www.vcrlter.virginia.edu/

Ozesmi, S. L., & Bauer, M. E. (2002). Satellite remote sensing of wetlands. *Wetlands Ecology and Management*, *10*, 381–402.

Pavri, F., & Aber, J. S. (2004). Characterizing wetland landscapes: A spatiotemporal analysis of remotely sensed data at Cheyenne Bottoms, Kansas. *Physical Geography*, *25*, 86–104.

Ramsey, E. W., & Laine, S. C. (1997). Comparison of Landsat Thematic Mapper and high resolution photography to identify change in complex coastal wetlands. *Journal of Coastal Research*, *13*, 281–292.

Rogers, A. S., & Kearney, M. S. (2004). Reducing signature variability in unmixing coastal marsh Thematic Mapper scenes using spectral indices. *International Journal of Remote Sensing*, *25*, 2317–2335.

Rundquist, D. C., Narumalani, S., & Narayanan, R. M. (2001). A review of wetlands remote sensing and defining new considerations. *Remote Sensing Reviews*, *20*, 207–226.

Sader, S. A., Ahl, D., & Liou, W. S. (1995). Accuracy of Landsat TM and GIS rule-based methods for forest wetland classification in Maine. *Remote Sensing of Environment*, *53*, 133–144.

Stolt, M. H., & Baker, J. C. (1995). Evaluation of National Wetland Inventory maps to inventory wetlands in the southern Blue Ridge of Virginia. *Wetlands*, *15*, 346–353.

Thomas, N. E. (2006). *Monitoring the spread of the aggressive invader, Phragmites australisM.A. scholarly paper.* College Park, MD: Department of Geography, University of Maryland.

Tiner, R. W. (1998). Trends in the Chesapeake Bay watershed wetlands. In M. J. Mac, P. A. Opler, C. E. P. Haeker, & P. D. Doran (Eds.), *Status and trends of the nation's biological resources* Reston, VA: U.S. Department of Interior, U.S. Geological Survey 964 pp.

Tiner, R. W. (2003). *Correlating enhanced National Wetlands Inventory data with wetland functions for watershed assessments: A rationale for northeastern U.S. wetlands.* Hadley, MA: U.S. Department of Interior, Fish and Wildlife Service, Northeast Region, National Wetlands Inventory Program 26 pp.

Tiner, R. W., Starr, M., Bergquist, H., & Swords, J. (2000). *Watershed-based wetland characterization for Maryland's Nanticoke River and Coastal Bays watersheds: A preliminary assessment report.*Hadley, MA: U.S. Department of Interior, Fish and Wildlife Service, Northeast Region, National Wetlands Inventory Program 73 pp.

Tockner, K., & Stanford, J. A. (2002). Riverine flood plains: Present state and future trends. *Environmental Conservation*, *29*, 308–330.

U.S. Fish and Wildlife Service (2006). *Wetlands online mapper.* Online: http://wetlandsfws.er.usgs.gov/

Weber, T. (2004). Landscape ecological assessment of the Chesapeake Bay watershed. *Environmental Monitoring and Assessment*, *94*, 39–53.

Wilen, B. O., & Bates, M. K. (1995). The U.S. Fish and Wildlife Service's National Wetlands Inventory project. *Vegetatio*, *118*, 153–169.

Zar, J. H. (1996). *Biostatistical analysis*, third ed. Upper Saddle River, NJ: Prentice-Hall 662 pp.